RESEARCH ARTICLE

Evaluation of Optimal Stimuli for SSVEP-Based Augmented Reality Brain-Computer Interfaces

SYEDA R. ZEHRA[1,2], (Graduate Student Member, IEEE), **JING MU**[1,2], (Member, IEEE),
BRANDON V. SYIEM[3], **ANTHONY N. BURKITT**[1], (Senior Member, IEEE),
AND DAVID B. GRAYDEN[1,2], (Senior Member, IEEE)

[1]Department of Biomedical Engineering, The University of Melbourne, Melbourne, VIC 3052, Australia
[2]Graeme Clark Institute for Biomedical Engineering, The University of Melbourne, Melbourne, VIC 3052, Australia
[3]School of Computer Science, Queensland University of Technology, Brisbane, QLD 4000, Australia

Corresponding author: Syeda R. Zehra (szehra@student.unimelb.edu.au)

ABSTRACT Steady-State Visually Evoked Potentials (SSVEPs) serve as one of the most robust Brain-Computer Interface (BCI) paradigms. Being an exogenous brain response, the properties of elicited SSVEPs are directly related to the properties of the visual stimuli. However, studies on integrating BCI and Augmented Reality (AR), aimed at realising mobile BCI systems, have mainly focused on applications of BCIs and performance comparison with screen-based BCIs. Little work has been done to study the effects of stimulus parameters on BCI performance when stimuli are presented with an AR headset. Here, we compare AR-based SSVEP with 3D and 2D stimuli using three different stimulation strategies: flickering, grow-shrink, and both. Participant feedback on level of fatigue and their subjective preference of stimuli were also collected. Our results did not show significant differences in classification accuracies between the 2D and 3D stimuli. However, for most of the participants, classification accuracy with flickering stimuli was above their average performance and stimuli that changed only in size were below average. The participants were divided in terms of which type of stimulus they felt was the most comfortable.

INDEX TERMS SSVEP, brain computer interface, augmented reality, 3D-stimuli, optical see-through.

I. INTRODUCTION

A Brain-Computer Interface (BCI) is a hardware and software communication tool that allows a person to control a device using recordings of brain activity alone [1]. BCI systems based on electroencephalography (EEG) are widely used in BCI research as they are easy to set up, non-invasive, and portable [2], [3].

While there are several BCI paradigms (for a review, see [4]), there has been a sharp increase in BCIs based on Steady-State Visually Evoked Potentials (SSVEPs) in the past

decade [5]. SSVEPs are oscillatory responses of the brain that entrain to the frequencies of repetitive periodic visual stimuli [6]. When a person looks at an object flickering at a particular frequency, this frequency and its harmonics can be detected in their cortical response, with strongest responses measured from the occipital region. Hence, multiple targets, each representing a command, can be presented via an SSVEP BCI by tagging each target with a unique frequency of presentation [7], [8]. When a user visually attends to a target, its frequency can be detected in their EEG and used to decode their intended target.

SSVEP BCIs are attractive because they require minimal user training, have high Information Transfer Rates

(ITRs) and usually do not require decoder calibration for each individual [9], [10], [11]. However, SSVEP responses depend upon many properties of the visual stimuli, such as size [12], [13], [14], color [15], contrast [12], [14], inter-stimulus distance [16], [17], [18], [19], [20], frequency [21], and the stimulator itself (Light-Emitting Diodes (LEDs), computer screen, etc.) [22]. Consequently, this is an active area of research and few commercial or clinical systems are currently available [23], [24], [25], [26].

The translation of SSVEP research to practical daily life applications requires investigation of mobile systems. Traditionally, to capture objects of interest in the same field-of-view as the stimuli, either LEDs are placed around the objects or a camera is used to capture the scene and present it on a computer screen along with the SSVEP stimuli. Both of these methods are limited in the number of objects and different scenarios that can be captured and presented. To this end, Augmented Reality (AR) combined with computer vision can be employed to tag any target objects in the user's field of view by superimposing SSVEP stimuli on them. Systems based on AR usually rely on a spatially aware (through multiple cameras placed on the headset), optical see-through display to project virtual content onto the real-world space. Augmented Reality (AR) has numerous benefits for real life, as it provides users with real-time interactive experiences wherein the real-world objects are enhanced and superimposed with computer-generated information across various sensory modalities, such as auditory, visual, and haptic. Interactions of BCIs with AR devices can enable direct brain interaction with the real world through AR; such as controlling movement of a robot [27], [28], [29] or virtual objects like a game avatar [30]. AR also complements BCIs well since users can receive real-time feedback of their intention while simultaneously executing a BCI command without needing to shift their gaze [31]. This property makes the systems more intuitive to use and suited to applications such as smart home control [32], [33], [34], [35] and rehabilitation [36].

So far, AR capabilities have not been fully utilized in SSVEP-BCI studies for visual stimulation. With see-through AR headsets, a wide range of two-dimensional (2D) and three-dimensional (3D) virtual content with control over their visual properties can be projected onto the real world. Since AR technology is relatively new to the BCI field, a substantial portion of studies relating to SSVEP-based BCIs have focused on BCI performance comparisons between computer screens and AR as visual stimulators [19], [28], [31], [37]. These studies have shown the performance of AR-BCI to be comparable to computer screens and the technology to be feasible for development of SSVEP-based AR-BCI.

There remains potential to design interactive and engaging stimulation paradigms with AR displays. One example is the grow-shrink stimulus introduced by Park et al. [33] that changed both size and luminance to improve classification accuracy in their 'smart-home' BCI. Modulation of stimulus size at a fixed frequency induces Steady-State Motion Visual Evoked Potentials (SSMVEP). When combined with modulation of brightness, both SSVEP and SSMVEP are induced, resulting in higher BCI accuracy. They used 2D tiles shaped as stars for stimulation. To our knowledge, only 2D planes/tiles have been used as stimuli in AR-BCI studies so far. But when viewed through the semi-transparent AR display, planes appear translucent and the user may easily lose attention and be distracted towards surrounding objects, which they can see through the projected ones [28]. The shift in gaze from the stimulus to the object behind it would potentially affect their BCI task performance.

Screen-based SSVEP studies have explored various stereo-scopic (3D) stimuli in comparison to planes/tiles (2D); however, use of holographic 3D stimuli for AR-BCI largely remains unexplored. Chien et al. [38] conducted a study on SSVEP in 3D displays on computer screens and reported that, if low disparity is maintained, stereoscopic 3D stimuli can lead to a higher degree of attention. It was observed by Mun et al. [39] that the 3D stimuli used in SSVEP-based BCI systems engaged users' attention and motivation while decreasing task response time. Another study conducted by Han et al. [40] concluded that stereoscopic motion stimulation elicits significantly higher amplitude SSVEP responses than its 2D counterpart. All of these comparison studies were conducted on computer screen displays and need to be validated with holographic virtual content. With AR displays, holographic 3D stimuli can be designed for eliciting SSVEP responses that are engaging, appear opaque through the head-mounted display (HMD), and may yield better performance compared to their 2D counterparts. Moreover, with 3D stimuli, the number of targets can be increased by anchoring stimuli spatially in 3D space. Targets separated cross-sectionally can be tagged with separate stimuli at different locations in the z-axis (distance from the user) but similar x and y coordinates (the horizontal and vertical visual planes, respectively) by appropriately adjusting their sizes to maintain the same visual angle for similar amplitude SSVEP responses [41]. Users can simply shift the focus of their gaze to select one of the targets [42], [43] located at different depths. However, no study has evaluated the BCI performance of 3D SSVEP stimuli in AR settings and it is unknown how these compare with 2D stimuli.

In this study, we compared 3D and 2D SSVEP stimuli using three different stimulation strategies for potential future BCI applications to draw comparisons between the two types of display for the HMD. We used flickering stimuli (i.e., brightness changing), size changing stimuli, and size-and-brightness changing stimuli. It has been reported in BCI user studies that the flashing of stimuli in SSVEP quickly fatigues the participants and prolonged exposure is often uncomfortable [44]. Therefore, alongside flashing stimuli, we included the stimuli that vary in size only during stimulation to compare performance of the two. User experience was collected in a post-experiment questionnaire to gauge

participants' fatigue and comfort while they performed the experiment.

II. MATERIALS AND METHODS

A. STIMULATION PARADIGM

There were six different types of stimuli used in the experiment, and for each stimulus there were two periodically changing characteristics: brightness and size. Three categories of stimuli were used with both 2D and 3D shapes: i. Flashing Stimulus (FS) that changed in brightness only, ii. Grow-Shrink Stimulus (GSS) that cycled between 1° and 6° in visual angle measured edge-to-edge, and iii. Grow-Shrink and Flashing Stimulus (GSFS) that simultaneously varied simultaneously in brightness and size. The GSFS exhibited maximum brightness at maximum size (6°) and minimum brightness at minimum size (1°). The visual stimulation paradigm was written using C# in the Unity 3D (Unity Technologies, USA) engine and was run on HoloLens version 2 (Microsoft Inc., Redmond, WA, USA).

Both brightness and size were modulated based on a sampled sinusoid,

$$s(f, t) = A \sin(2\pi f t) + c, \tag{1}$$

where s is a stimulus property (i.e., brightness and/or size) at frequency f and time t, A is the peak to peak amplitude of the stimulus, and c is the offset that determines the minimum brightness or size. For size changing stimuli, size changed in all of the defined (2D or 3D) dimensions. The stimuli shapes and layout are shown in Fig. 1. The size of FS was set to the mean of the maximum and minimum cross-sectional areas of GSFS for both 2D and 3D FS, which was 4.46° in visual angle.

B. PARTICIPANTS

Twelve healthy participants (7 females, 5 males) with normal or corrected-to-normal (with glasses or contact lenses) vision volunteered to take part in this research study. This study was approved by the University of Melbourne Human Research Ethics Committee (Approval Number 2057895). Signed written consent was obtained from each participant prior to commencement.

C. TIMING AND FREQUENCY

Five integer stimulus frequencies, 12, 13, 14, 15, 16 Hz, were used. We deliberately avoided frequencies in the lower alpha band (8-11 Hz) to avoid the influence of spontaneous alpha activity. The five stimuli were equidistantly placed on a transparent circle that measured 10° in diameter with their centers lying on the circumference, as shown in Fig. 1(a). The center of this circle was fixed to the center of the participant's field of view (FOV) at the start of the experiment and remained at the same position throughout the experiment. This configuration was chosen to make the experimental setting closer to a real-world scenario, where objects are usually stationary.

Four trials were recorded for each frequency, totaling 20 trials for each type of stimulus. All participants were tested
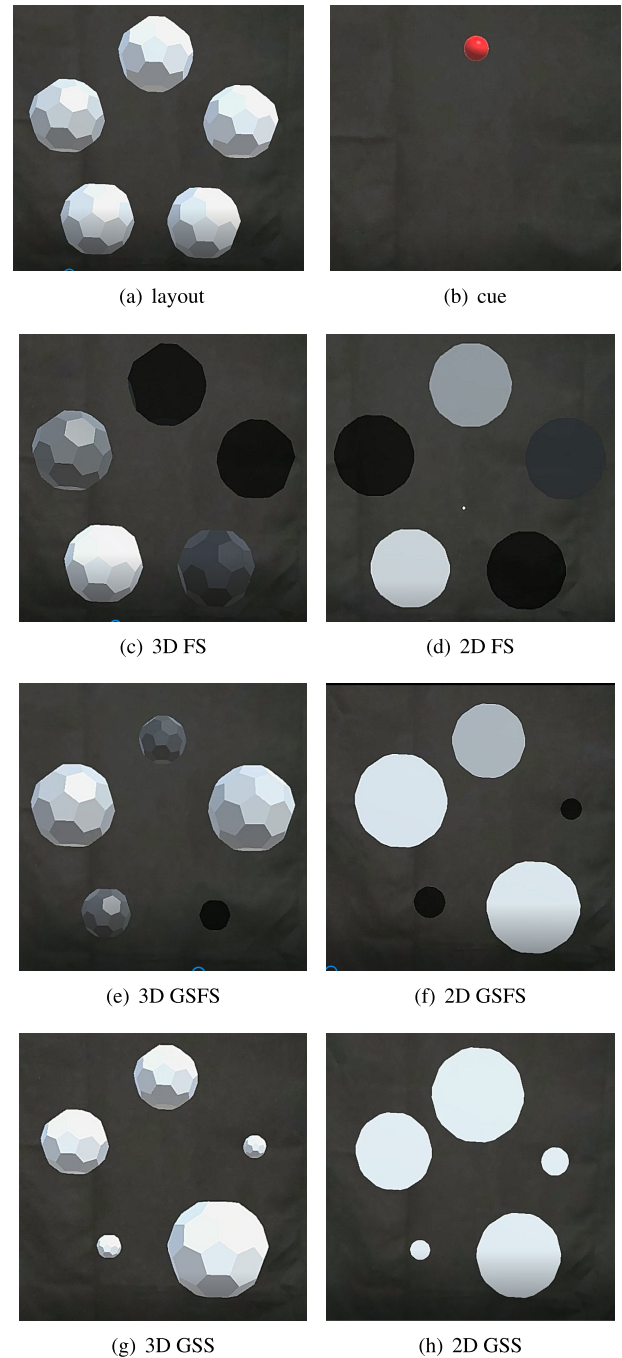

(a) layout (b) cue

(c) 3D FS (d) 2D FS

(e) 3D GSFS (f) 2D GSFS

(g) 3D GSS (h) 2D GSS

FIGURE 1. Stimuli layout used in the experiment. (a) The layout of the five different frequencies in space. (b) Cue for each trial that was placed in the location of the stimulus to attend to. Screenshots of (c) 3D FS stimlul, (d) 3D GSS stimuli, (e) 3D GSFS stimuli, (f) 2D FS stimuli, (g) 2D GSS stimuli and (h) 2D GSFS stimuli.

for the six types of stimuli, as illustrated in Fig. 1(c-h), which totaled 120 trials recorded from each participant. The timing of each trial is shown in Fig. 2(a). All the trials and blocks were randomised across participants. The participant was shown a cue, a small red sphere, that appeared for 0.75 s at the position of the target stimulus (Fig. 1(b)). Participants were asked to keep looking at the cue location, which was then
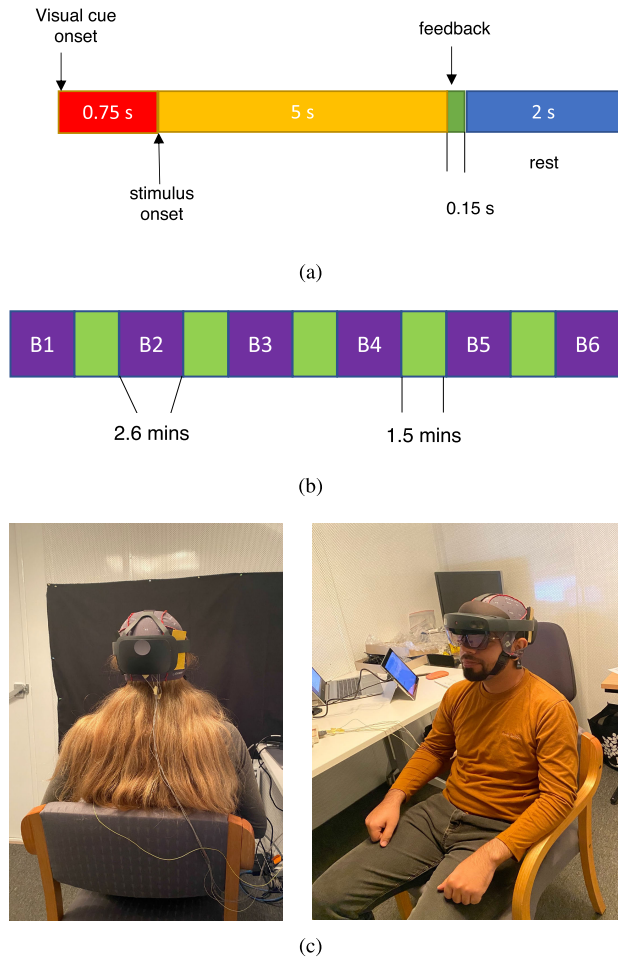
(a)

(b)

(c)

FIGURE 2. a) Timing within a trial. b) Duration of blocks within the experiment. c) Back and front views of the experimental setup.

replaced with a white stimulus shown for 5 s concurrently with the other four non-target stimuli. After the stimulus presentation finished, auditory feedback (duration 0.15 s) was provided to participants: a short melody was played if the target frequency was correctly detected in the EEG signal and a buzzing sound was played if the target frequency was not correctly detected. The purpose of the feedback was to retain user engagement and help them focus on the experimental task. A rest period of 2 s followed the feedback.

Fig. 2(b) shows the time distribution across the different blocks of the experiment. The experiment was split into six blocks to provide regular breaks. During each block, all the trials of only one type of stimulus were presented. The sequence of stimuli blocks and target frequencies in trials were both randomised for each participant to minimise order effects. A break of 1.5 min was provided between consecutive blocks (Fig. 2(b)).

D. HARDWARE SETUP AND SYSTEM ARCHITECTURE
EEG was recorded in a Faraday shielded room with g.USBamp and g.Sahara dry electrodes (g.tec medical engineering GmbH, Austria) sampled at 512 Hz. A notch filter at 50 Hz for removal of line-noise and a bandpass filter

TABLE 1. Response scale used in the questionnaire.

1	2	3	4	5
not at all	somewhat	moderately	very	extremely

with 0.5-60 Hz pass band were applied in the g.USBamp's data acquisition software package during EEG recording. EEG was measured at six electrode sites according to the 10-20 international system: PO3, POz, PO4, O1, Oz and O2. Long leg electrodes were used for participants with thick hair and short leg electrodes for others to ensure good contact with the skin. Reference and ground were placed on the right mastoid and left mastoid, respectively, using adhesive electrodes.

Participants sat approximately 1 m from a black background, measured at their eye level (Fig. 2(c)). After fitting the EEG cap and electrodes, participants wore the HoloLens over the top of the EEG cap and electrodes. Foam padding was inserted at the sides to prevent the HoloLens from pressing onto the electrodes. It was ensured that participants were comfortable throughout the experiment by verbally asking them during the breaks.

SSVEP stimuli were projected using the HoloLens, rendered at a frame rate of 60 Hz. To ensure that the augmented projections of stimuli were presented at the intended locations, the HoloLens was calibrated to each participant's eyes using a built-in calibration routine. Event triggers were sent to a Windows PC from HoloLens as UDP packets via Wi-Fi and were received in a Simulink (MathWorks Inc., USA) model recording the EEG.

E. QUESTIONNAIRE
At the end of the experiment, participants were asked to complete a questionnaire to report their subjective evaluation of fatigue and experience wearing the HoloLens and EEG dry electrodes for the duration of the experiment. The questions asked were:

1) Was the flickering of the stimulus annoying?
2) Was the flickering of the stimulus fatiguing?
3) How strenuous was the experimental task using the HoloLens device?
4) Do you feel any discomfort in the eyes?
5) Did you feel dizzy?
6) Which stimulus were you the most comfortable with?
7) Would you be comfortable using the HoloLens if the experiment extended for more than an hour?

Questions 4, 5, and 7 required a binary response while the other questions' responses were recorded on a five-point scale as shown in Table 1.

F. DATA ANALYSES
1) ONLINE PROCESSING
During the experiment, event triggers sent via UDP to the MATLAB Simulink model identified the five second EEG segments related to the SSVEP response. Each segment was stored in a buffer and decoded using Canonical Correlation

Analysis (CCA) [45] at the end of the stimulation period to provide online auditory feedback to the participant during the experiment. All six electrode channels were used for online decoding.

2) OFFLINE PROCESSING

Epochs of 5 s duration of EEG corresponding to stimulation periods were extracted using the event triggers that labelled the start and end of the stimulation. The data were band-pass filtered with a pass-band between 6 and 60 Hz using the 'bandpass' function in MATLAB with 'ImpulseResponse' set to 'auto', 'Steepness' set to 0.85, and 'StopbandAttenuation' set to 60 dB. During the post-processing of EEG data, unexpected 15 Hz and 30 Hz noise were observed on some channels that substantially reduced the classification accuracy, as 15 Hz is also a stimulation frequency tested in this experiment. The channels with this noise were not consistent amongst participants. To avoid the effect of this noise, a combination of three optimal electrodes was determined for each participant using the approach adopted by Park et al. [33] to remove the majority, if not all, channels that were contaminated: for each participant, classification accuracy for all possible combination of three electrodes was calculated, the electrode combination that yielded highest classification accuracy was selected as the optimal electrode combination and used for offline analysis.

3) CANONICAL CORRELATION ANALYSIS

Canonical Correlation Analysis (CCA) was used for decoding. For SSVEP classification, the two inputs for the CCA algorithm were the processed EEG trial data and a set of reference signals Y_f composed of sine and cosine waves of the fundamental stimulation frequency f and its harmonics [45],

$$Y_f = \begin{pmatrix} \sin(2\pi f t) \\ \cos(2\pi f t) \\ \vdots \\ \sin(2\pi n_h f t) \\ \cos(2\pi n_h f t) \end{pmatrix}, \quad (2)$$

where n_h is the number of harmonics included in the reference set. The CCA algorithm determines a set of linear combinations of the two inputs such that the correlation between them is maximised. This process was repeated using a reference signal set for each frequency and the correlation coefficient was determined. The frequency yielding the highest correlation with the EEG trial data was selected as the frequency decoded for that trial. Performance evaluation metrics were calculated from results of performing CCA on all trials.

G. PERFORMANCE EVALUATION

Performance in this study was evaluated using target Classification Accuracy (CA) and Information Transfer Rate (ITR). The ITR, B, as defined by McFarland and Wolpaw [46] is:

$$B = \frac{60}{T}\left(\log_2 N + P\log_2 P + (1-P)\log_2\left[\frac{1-P}{N-1}\right]\right), \quad (3)$$

TABLE 2. Selected optimal combination of three electrode channels used for offline analysis for each participant.

Participant	Electrode combination
P1	PO3 , O1 , Oz
P2	Pz , PO4 , O2
P3	PO3 , PO4 , O1
P4	PO3 , Pz , PO4
P5	PO3 , Pz , Oz
P6	Pz , PO4 , Oz
P7	PO4 , Oz , O2
P8	Pz , PO4 , Oz
P9	Pz , PO4 , Oz
P10	PO3 , Pz , O1
P11	PO3 , Pz , PO4
P12	PO4 , O1 , O2

in bits/min, where N is the total number of possible outcomes, P is the probability of selecting the desirable output (i.e., classifier accuracy), and T is the total time required to make a selection.

H. STATISTICAL ANALYSIS

The Kolmogorov-Smirnov test confirmed that participants' classification accuracies followed a normal distribution. A Linear Mixed Effects (LME) model was fitted on classification accuracies with a fixed effect of stimulus and a random effect of participant to capture the variability within the participants and assess the overall effect of type of stimulus on BCI performance. One-way ANOVA was performed on the LME model and subsequent pairwise comparisons were carried out to investigate the differences between individual stimuli for statistical significance, with Tukey adjustment for multiple comparisons.

III. RESULTS

For offline analysis, the combination of three electrodes optimised by classification accuracy was used. Table 2 lists the best combination of three channels identified based on the CA for each participant. Each participant's classification accuracy with all types of stimuli are plotted in Fig. 3. The plot highlights both inter-participant and intra-participant variability. For each participant, the stimulus they reported as the most comfortable to view in the questionnaire (Table 4) is marked with a cross ('x') on the plot. High accuracy for a stimulus type corresponds with the preferred choice of stimulus for some participants, such as Participants 6 and 12, but did not match for most of the participants. For the majority of the participants, classification accuracy for GSS stimulus was lower than their performance for other stimuli.

The average CA of each participant was also evaluated (Fig. 4), which showed large variation between the participants. Fig. 5 shows the differences of each participant's average classification accuracy for each type of stimuli from their own mean performance. For both 3D and 2D FS, most participants performed better than their average accuracy, while CA was below average for the majority of the participants with 3D and 2D GSS.
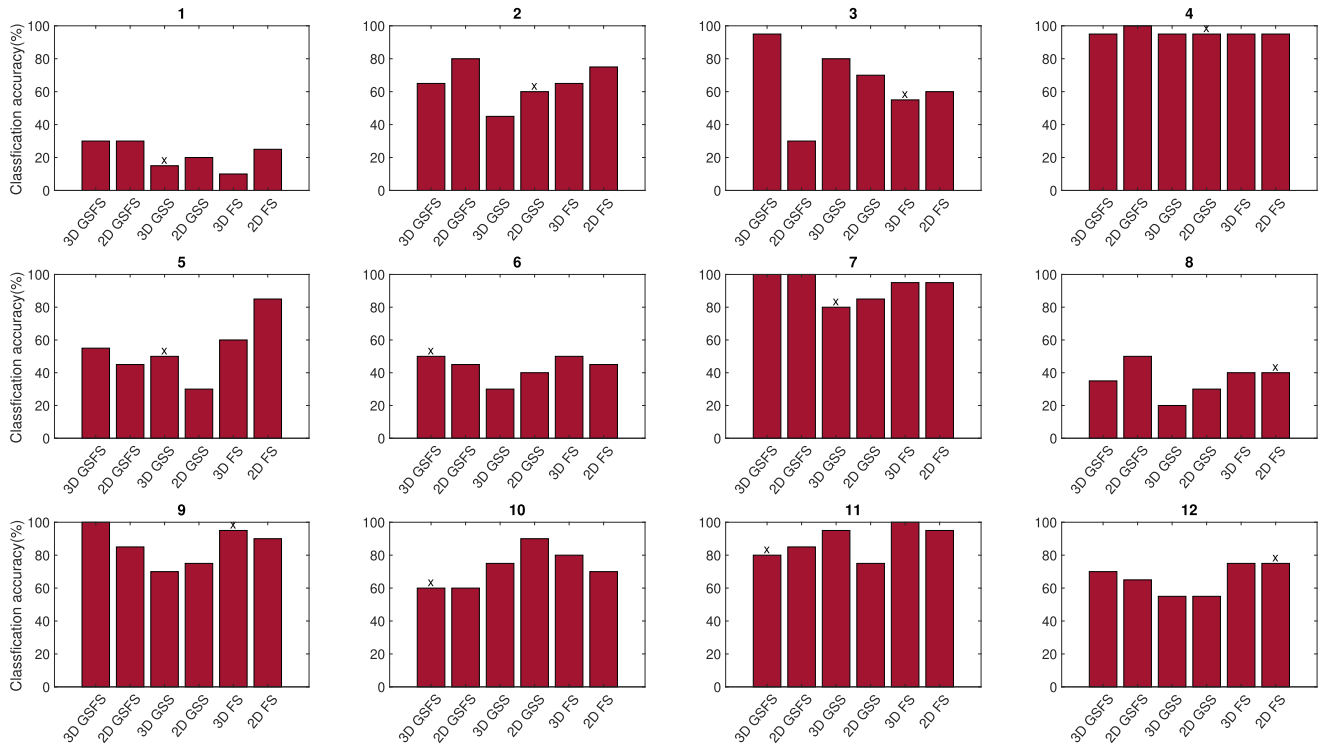
FIGURE 3. Average classification accuracies for all participants for each type of stimulus using three optimal electrodes. The 'x' indicates each participant's preferred stimulus chosen in the post-experiment questionnaire.
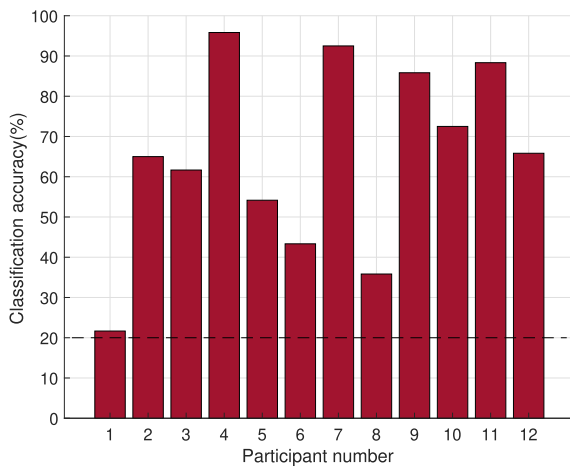

FIGURE 4. Average classification accuracy for each participant across all trials. Chance level is shown by the dashed line.
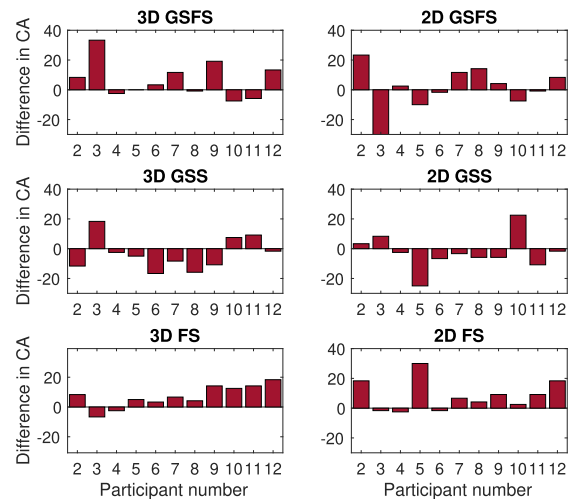

FIGURE 5. The differences between each participant's classification accuracies for each type of stimulus and their average classification accuracy.

To avoid introduction of a bias in statistical tests, Participant 1 was removed from statistical analyses since their classification accuracy was only at the chance level (20%), as shown in Fig. 4 (dashed line), and so was considered an outlier.

To evaluate the performance of the different types of stimuli, average classification accuracy of each stimulus over all trials was calculated for Participants 2-12 (Fig. 6). 3D GSFS, 3D FS, and 2D FS yielded the highest accuracies. Classifi-

cation accuracies for 2D and 3D GSS were lower than other types of stimuli. One-way ANOVA of classification accuracy with participants and stimuli as factors showed no significant differences between stimuli ($F(5,50) = 2.13$, $p = 0.077$). Subsequent post-hoc pairwise comparisons performed on the linear mixed model of the classification accuracies, where participants were kept as a random effect, also did not reveal

TABLE 3. P-values for pairwise comparisons on the linear mixed effects model on CA of the six stimuli.

	3D GSFS	2D GSFS	3D GSS	2D GSS	3D FS	2D FS
3D GSFS	-	-	-	-	-	-
2D GSFS	0.883	-	-	-	-	-
3D GSS	0.357	0.942	-	-	-	-
2D GSS	0.464	0.978	1.00	-	-	-
3D FS	1.00	0.843	0.309	0.409	-	-
2D FS	0.99	0.694	0.189	0.264	1.00	-
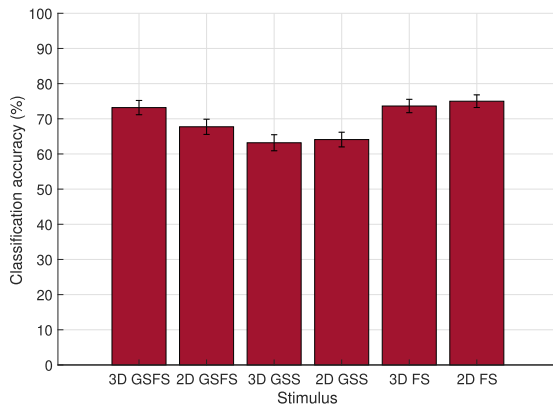
FIGURE 6. Average classification accuracy for each type of stimulus. The error bars represent standard error. sg differences.
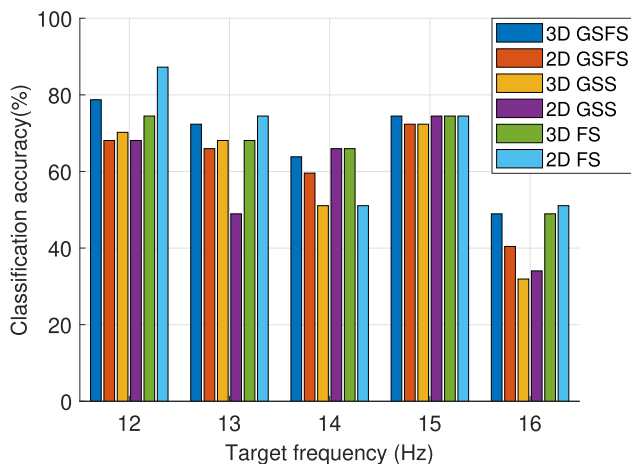
FIGURE 7. Average classification accuracy at each frequency for each stimulus.

any significant differences between the six types of stimuli or any of the 2D and 3D pairs (Table 3). However, upon carefully reading the p-values from multiple comparisons, GSS yields much lower p-values when compared with FS than other pairwise comparisons.

Frequency is an important factor that affects the performance of SSVEP-BCI. In Fig. 7, the average classification accuracies of all five frequencies yielded by each stimulation strategy are plotted. As found in previous work, accuracy tended to decline with increasing frequency [47], [48], [49], [50].
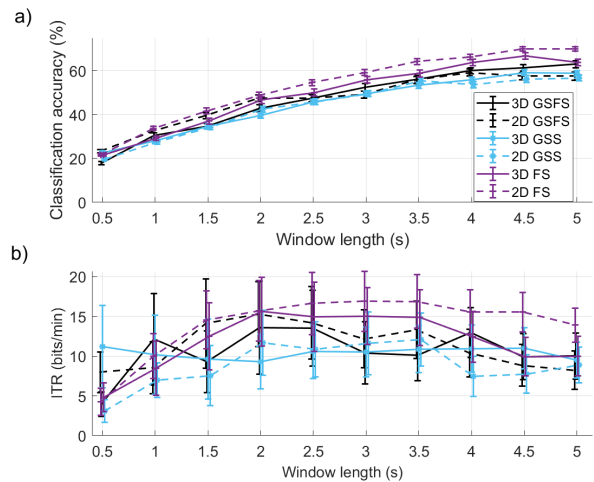
FIGURE 8. Average (a) Classification Accuracy (CA) and (b) Information Transfer Rate (ITR) for each stimulus with increasing window lengths in decoding. The error bars represent standard error.

Time taken to accurately decode an EEG signal and produce a system outcome indicates the potential response rate and practicality of a BCI system. For evaluation of the optimal stimulation time for each type of stimulus, the average CA was calculated for all participants using time windows of 0.5 s to 5 s in steps of 0.5 s (Fig. 8). The results show that the 2D and 3D pairs of GSS and GSFS both yielded approximately the same classification accuracies for all window lengths except 0.5 s. CA for 2D-FS increased at a steeper rate than other types and it yielded the same average accuracy at 3 s as 2D-GSS and 3D-GSS showed at 5 s. After 3.5 s, both 3D and 2D-FS had similar CA. Overall, 2D-FS achieved the best classification accuracy and ITR for most window lengths while GSS was the poorest.

The responses of the post-experiment questionnaire are tabulated in Table 4. In the questionnaire, five out of the 12 participants reported 2D or 3D GSS as their preferred choice of stimulus. Similarly, five out of 12 participants reported FS and two reported 3D GSFS as their preferred stimulus. No participant marked 2D GSFS as the stimulus of their choice in terms of visual comfort. Furthermore, eight out of 12 participants reported post-experiment fatigue (responses 3-5) while the remaining four did not report experiment-related fatigue (responses 1-2). Except for Participant 11, no participant agreed to wear the dry electrodes and HoloLens for any longer than the duration of the experiment, which ranged from 50-70 minutes.

IV. DISCUSSION
A. PERFORMANCE COMPARISON OF 2D AND 3D STIMULI
The performance of three types of 2D and 3D stimuli were evaluated in this study. For a given stimulation paradigm, both 2D and 3D stimuli yielded similar performance for all time windows of classification accuracies (CA) and information transfer rate (ITR). Slightly larger differences in performance

TABLE 4. Post-experiment questionnaire responses.

Participant number	flickering felt annoying	fatigued after experiment	task felt strenuous	eye discomfort	feel dizzy	would wear HL for longer	most comfortable stimulus
P1	2	2	1	No	No	No	3D GSS
P2	4	3	3	No	No	No	2D GSS
P3	2	3	2	No	No	No	3D FS
P4	5	5	4	No	No	No	2D GSS
P5	3	4	1	No	No	No	3D GSS
P6	2	2	2	Yes	No	No	3D GSFS
P7	2	3	2	No	No	No	3D GSS
P8	2	1	1	No	No	No	2D FS
P9	4	4	4	Yes	No	No	3D FS
P10	2	2	3	No	No	No	2D FS
P11	4	3	2	Yes	No	Yes	3D GSFS
P12	2	3	2	Yes	No	No	2D FS

were observed for the Flashing Stimulus (FS) in terms of both CA and ITR. 2D-FS yielded higher average CA than 3D-FS for time intervals of less than 4 s. Similarly, for window lengths of less than 2.5 s with Grow-Shrink and Flashing Stimulus (GSFS), 2D-GSFS showed higher CA than 3D-GSFS. However, these differences were not statistically significant. We speculate that this may be because the 2D and 3D stimuli both cover the same area in the visual field, which has higher impact on the evoked response as compared to adding the third dimension in the stimuli and, hence, the visually evoked responses do not differ significantly. It is also not evident from questionnaire responses whether 2D or 3D was consistently considered more comfortable than the other amongst participants. However, we have demonstrated in this experiment that both 2D and 3D variants of a particular strategy would yield similar BCI performance.

B. PERFORMANCE COMPARISON OF STIMULATION STRATEGIES

In terms of comparison of three stimulation strategy, CA is consistently lower for stimuli that change in size only (Grow-Shrink Stimulus, GSS). GSS elicits Steady-State Motion Visual Evoked Potentials (SSMVEP) only and while it was the preferred choice for 40% of the participants, the evoked response was less accurately decoded. In contrast, the decoding results from FS and GSFS were comparable to one another, and no significant differences were found between the two, contrary to the results reported by Park et al. [33] who reported GSFS to perform significantly better than FS.

The overall mean accuracy in this study was also lower than the values reported by Park et al. The discrepancy observed in our experiment from Park et al.'s could be due to the use of dry electrodes and the layout of stimuli and absence of a fixation point. In a study with 102 participants, Zhu et al. [51] showed that CA for the same stimulation conditions in SSVEP using dry electrodes can differ by up to 20% from wet electrodes. In this experiment, the overall average accuracy for GSFS at 5 s of stimulation was 75.2% compared to 92.8% achieved by Park et al., in accordance with Zhu et al.'s conclusion. Another SSVEP-BCI system tested by Farmaki et al. [52] who used dry electrodes for recording three channel SSVEP

reported an average accuracy of 80.2% and lowest accuracy of 46%. Although, dry electrodes facilitate easy placement and removal of EEG electrodes, the technology still requires improvement to match the output of wet electrodes.

Secondly, the placement and composition of targets also affect accuracy. In our study, the stimuli were placed equidistantly on a circle. For a size changing stimulus, the motion of the stimulus is perceived as the adjacent stimuli grow and shrink in size. Distraction caused by a moving object in the periphery of the target stimulus is greater for the participants compared to a stationary flickering object, especially when there is no focus point to direct their attention towards the target during stimulation. The moving adjacent stimuli appear to be coming closer and moving further away from the target and may divert the participant's attention. The superimposed pictures of home appliances on stimuli in Park et al.'s study also act as anchoring points for participant attention, thereby enhancing performance for GSFS. SSVEP-AR studies that report high classification accuracy are application-based meaning the different stimuli presented are associated with different commands. For example, Ke et al. [28] used eight SSVEP targets to control a robotic arm similar to Zhang et al. [27] who both reported accuracies above 90%. Associating a stimulus with a task can help user retain their attention.

C. QUESTIONNAIRE RESULTS

An important finding from the questionnaire was the reluctance of participants to wear the head-mounted display on top of dry electrodes for longer duration. This response was independent of experiment-induced fatigue. Participants who did not report fatigue also disapproved of wearing the headset for long duration. The bulkiness of the HoloLens and the shape of dry electrodes both contribute to this. As the dry electrodes make contact with the scalp through thin cylindrical legs, a small amount of force pushing onto the electrodes translates into large pressure at the back of the head leading to discomfort. Although foam padding was inserted during the experiment to create a gap between the headset and the electrodes, the overall experience was still unpleasant for the majority of the participants. This indicates that the

combination of dry electrodes with head mounted displays is not ideal for a long duration and wet electrodes may be better suited.

D. EFFECT OF FREQUENCY

In terms of CA, 3D GSFS and 3D FS were most stable amongst all stimuli and yielded consistent performance for 12-15 Hz. When evaluated for each stimulation frequency, CA varied considerably. As observed in Fig. 7, average CA decreased as the frequency increased except at 15 Hz where the CA rose and had almost the same average value across all the stimuli. It is worth noting that 15 Hz is also a dividend of the Hololens's refresh rate of (60 Hz), which may have impacted the EEG recording. However, studies on SSVEP frequencies with stimulation frequencies in the range of 12-18 Hz have shown that a local maximum in the EEG power distribution is typically observed around 15 Hz [13], [53]. Classification accuracy at the maximal frequency of 16 Hz was lowest for all stimuli following the decreasing pattern of accuracy with increasing frequency. Our results are consistent with the studies in the literature who also reported decrease in CA or signal-to-noise ratio for increasing stimulation frequency beyond 10 Hz [47], [48], [49], [50].

E. FUTURE WORK

Using AR displays, 3D stimuli can be laid out and anchored in 3D space to increase the number of stimuli presented simultaneously. Future experiments could explore a presentation setup where stimuli are anchored at different viewing distances from the participant. Previous experiments with a set of LEDs have shown that the two SSVEP targets placed at different depths in a single direction of view can elicit distinguishable cortical responses [42]. By spacing out stimuli in all three dimensions of space, the number of simultaneous targets can be increased. Multiple colors could be used to improve discernability between targets hence improving the classification accuracy.

One of the limitations in this study was the use of integer frequencies ranging to the higher end frequencies that yielded lower accuracies. The performance can be further improved by testing multiple frequencies (integer and non-integer values) to identify a set of frequencies that yields the strongest response and higher accuracy.

V. CONCLUSION

Stimuli properties determine the strength and quality of exogenous brain responses. The main advantages of AR technology for SSVEP-based BCIs are system portability and incorporation with a person's surroundings. The combination of the two requires an engaging stimulation paradigm within concise layouts. In this study, we evaluated the use of dry electrodes and an optically see-through head mounted display, finding that both 3D and 2D single graphic SSVEP stimuli yielded similar participant performance and may be used for designing BCI experiments. However, for

stimulation periods of less than 3.5 s, flickering stimulus gave higher accuracy and information transfer rate.

REFERENCES

[1] J. Wolpaw, N. Birbaumer, D. McFarland, G. Pfurtscheller, and T. Vaughan, "Brain-computer interfaces for communication and control," *Clin. Neurophys.*, vol. 113, no. 6, pp. 767–791, 2002.

[2] L. F. Nicolas-Alonso and J. Gomez-Gil, "Brain computer interfaces, a review," *Sensors*, vol. 12, no. 2, pp. 1211–1279, 2012.

[3] W. Zhang, C. Tan, F. Sun, H. Wu, and B. Zhang, "A review of EEG-based brain-computer interface systems design," *Brain Sci. Adv.*, vol. 4, no. 2, pp. 156–167, Dec. 2018.

[4] R. Abiri, S. Borhani, E. W. Sellers, Y. Jiang, and X. Zhao, "A comprehensive review of EEG-based brain–computer interface paradigms," *J. Neural Eng.*, vol. 16, no. 1, 2019, Art. no. 011001.

[5] Y. Zhang, S. Q. Xie, H. Wang, and Z. Zhang, "Data analytics in steady-state visual evoked potential-based brain–computer interface: A review," *IEEE Sensors J.*, vol. 21, no. 2, pp. 1124–1138, Jan. 2021.

[6] N. R. Galloway, "Human brain electrophysiology: Evoked potentials and evoked magnetic fields in science and medicine," *Brit. J. Ophthalmol.*, vol. 74, no. 4, p. 255, Apr. 1990.

[7] M. Li, D. He, C. Li, and S. Qi, "Brain–computer interface speller based on steady-state visual evoked potential: A review focusing on the stimulus paradigm and performance," *Brain Sci.*, vol. 11, no. 4, p. 450, Apr. 2021.

[8] A. Rezeika, M. Benda, P. Stawicki, F. Gembler, A. Saboor, and I. Volosyak, "Brain–computer interface spellers: A review," *Brain Sci.*, vol. 8, no. 4, p. 57, Mar. 2018.

[9] M. Nakanishi, Y. Wang, Y.-T. Wang, and T.-P. Jung, "A comparison study of canonical correlation analysis based methods for detecting steady-state visual evoked potentials," *PLoS ONE*, vol. 10, no. 10, Oct. 2015, Art. no. e0140703.

[10] J. Jiang, E. Yin, C. Wang, M. Xu, and D. Ming, "Incorporation of dynamic stopping strategy into the high-speed SSVEP-based BCIs," *J. Neural Eng.*, vol. 15, no. 4, Aug. 2018, Art. no. 046025.

[11] X. Chen, Y. Wang, M. Nakanishi, X. Gao, T.-P. Jung, and S. Gao, "High-speed spelling with a noninvasive brain–computer interface," *Proc. Nat. Acad. Sci. USA*, vol. 112, no. 44, pp. E6058–E6067, Nov. 2015.

[12] J. Bieger, G. G. Molina, and D. Zhu, "Effects of stimulation properties in steady-state visual evoked potential based brain-computer interfaces," in *Proc. 32nd Annu. Int. Conf. IEEE Eng. Med. Biol. Soc.*, 2010, pp. 3345–3348.

[13] K. B. Ng, A. P. Bradley, and R. Cunnington, "Stimulus specificity of a steady state visual evoked potential-based brain–computer interface," *J. Neural Eng.*, vol. 9, no. 3, 2012, Art. no. 036008.

[14] A. Duszyk, M. Bierzyńska, Z. Radzikowska, P. Milanowski, R. Kuś, P. Suffczyński, M. Michalska, M. Łabęcki, P. Zwoliński, and P. Durka, "Towards an optimization of stimulus parameters for brain-computer interfaces based on steady state visual evoked potentials," *PLoS ONE*, vol. 9, no. 11, Nov. 2014, Art. no. e112099.

[15] Y. Du and X. Zhao, "Visual stimulus color effect on SSVEP-BCI in augmented reality," *Biomed. Signal Process. Control*, vol. 78, Sep. 2022, Art. no. 103906.

[16] K. B. Ng, A. P. Bradley, and R. Cunnington, "Effect of competing stimuli on SSVEP-based BCI," in *Proc. Annu. Int. Conf. IEEE Eng. Med. Biol. Soc.*, Aug. 2011, pp. 6307–6310.

[17] S. Fuchs, S. K. Andersen, T. Gruber, and M. M. Müller, "Attentional bias of competitive interactions in neuronal networks of early visual processing in the human brain," *NeuroImage*, vol. 41, no. 3, pp. 1086–1101, Jul. 2008.

[18] J. Mu, D. B. Grayden, Y. Tan, and D. Oetomo, "Spatial resolution of visual stimuli in SSVEP-based brain-computer interface," in *Proc. 9th Int. IEEE/EMBS Conf. Neural Eng. (NER)*, Mar. 2019, pp. 928–932.

[19] X. Zhao, C. Liu, Z. Xu, L. Zhang, and R. Zhang, "SSVEP stimulus layout effect on accuracy of brain-computer interfaces in augmented reality glasses," *IEEE Access*, vol. 8, pp. 5990–5998, 2020.

[20] R. Zhang, Z. Xu, L. Zhang, L. Cao, Y. Hu, B. Lu, L. Shi, D. Yao, and X. Zhao, "The effect of stimulus number on the recognition accuracy and information transfer rate of SSVEP–BCI in augmented reality," *J. Neural Eng.*, vol. 19, no. 3, May 2022, Art. no. 036010.

[21] D. Regan, *Human Brain Electrophysiology: Evoked Potentials and Evoked Magnetic Fields in Science and Medicine*. Amsterdam, The Netherlands: Elsevier, 1989.

[22] J. Mu, D. B. Grayden, Y. Tan, and D. Oetomo, "Comparison of steady-state visual evoked potential (SSVEP) with LCD vs. LED stimulation," in *Proc. 42nd Annu. Int. Conf. IEEE Eng. Med. Biol. Soc. (EMBC)*, Jul. 2020, pp. 2946–2949.

[23] Q. Gao, X. Zhao, X. Yu, Y. Song, and Z. Wang, "Controlling of smart home system based on brain-computer interface," *Technol. Health Care*, vol. 26, pp. 1–15, Jul. 2018.

[24] X. Zeng, G. Zhu, L. Yue, M. Zhang, and S. Xie, "A feasibility study of SSVEP-based passive training on an ankle rehabilitation robot," *J. Healthcare Eng.*, vol. 2017, pp. 1–9, Sep. 2017.

[25] M. Adams, M. Benda, A. Saboor, A. F. Krause, A. Rezeika, F. Gembler, P. Stawicki, M. Hesse, K. Essig, S. Ben-Salem, Z. Islam, A. Vogelsang, T. Jungeblut, U. Ruckert, and I. Volosyak, "Towards an SSVEP-BCI controlled smart home," in *Proc. IEEE Int. Conf. Syst., Man Cybern. (SMC)*, Oct. 2019, pp. 2737–2742.

[26] C. J. Perera, I. Naotunna, C. Sadaruwan, R. A. R. C. Gopura, and T. D. Lalitharatne, "SSVEP based BMI for a meal assistance robot," in *Proc. IEEE Int. Conf. Syst., Man, Cybern. (SMC)*, Oct. 2016, pp. 2295–2300.

[27] S. Zhang, Y. Chen, L. Zhang, X. Gao, and X. Chen, "Study on robot grasping system of SSVEP-BCI based on augmented reality stimulus," *Tsinghua Sci. Technol.*, vol. 28, no. 2, pp. 322–329, Apr. 2023.

[28] Y. Ke, P. Liu, X. An, X. Song, and D. Ming, "An online SSVEP-BCI system in an optical see-through augmented reality environment," *J. Neural Eng.*, vol. 17, no. 1, Feb. 2020, Art. no. 016066.

[29] L. Chen, P. Chen, S. Zhao, Z. Luo, W. Chen, Y. Pei, H. Zhao, J. Jiang, M. Xu, Y. Yan, and E. Yin, "Adaptive asynchronous control system of robotic arm based on augmented reality-assisted brain–computer interface," *J. Neural Eng.*, vol. 18, no. 6, Nov. 2021, Art. no. 066005.

[30] K.-M. Choi, S. Park, and C.-H. Im, "Comparison of visual stimuli for steady-state visual evoked potential-based brain-computer interfaces in virtual reality environment in terms of classification accuracy and visual comfort," *Comput. Intell. Neurosci.*, vol. 2019, pp. 1–7, Jul. 2019.

[31] H. Si-Mohammed, J. Petit, C. Jeunet, F. Argelaguet, F. Spindler, A. Évain, N. Roussel, G. Casiez, and A. Lecuyer, "Towards BCI-based interfaces for augmented reality: Feasibility, design and evaluation," *IEEE Trans. Vis. Comput. Graphics*, vol. 26, no. 3, pp. 1608–1621, Mar. 2020.

[32] S. Park, J. Ha, J. Park, K. Lee, and C.-H. Im, "Brain-controlled, AR-based home automation system using SSVEP-based brain-computer interface and EOG-based eye tracker: A feasibility study for the elderly end user," *IEEE Trans. Neural Syst. Rehabil. Eng.*, vol. 31, pp. 544–553, 2023.

[33] S. Park, H.-S. Cha, J. Kwon, H. Kim, and C.-H. Im, "Development of an online home appliance control system using augmented reality and an SSVEP-based brain-computer interface," in *Proc. 8th Int. Winter Conf. Brain-Comput. Interface (BCI)*, Feb. 2020, pp. 1–2.

[34] F. Putze, D. Weiß, L.-M. Vortmann, and T. Schultz, "Augmented reality interface for smart home control using SSVEP-BCI and eye gaze," in *Proc. IEEE Int. Conf. Syst., Man Cybern. (SMC)*, Oct. 2019, pp. 2812–2817.

[35] S. Zhong, Y. Liu, Y. Yu, J. Tang, Z. Zhou, and D. Hu, "A dynamic user interface based BCI environmental control system," *Int. J. Human–Comput. Interact.*, vol. 36, no. 1, pp. 55–66, Jan. 2020.

[36] Y. Liu, Y. Liu, J. Tang, E. Yin, D. Hu, and Z. Zhou, "A self-paced BCI prototype system based on the incorporation of an intelligent environment-understanding approach for rehabilitation hospital environmental control," *Comput. Biol. Med.*, vol. 118, Mar. 2020, Art. no. 103618.

[37] E. Klein, T. Brown, M. Sample, A. R. Truitt, and S. Goering, "Engineering the brain: Ethical issues and the introduction of neural devices," *Hastings Center Rep.*, vol. 45, no. 6, pp. 26–35, Nov. 2015.

[38] Y.-Y. Chien, C.-Y. Lee, F.-C. Lin, Y.-P. Huang, L.-W. Ko, and H.-P. D. Shieh, "Research on steady-state visual evoked potentials in 3D displays," *Proc. SPIE*, vol. 9495, pp. 175–181, May 2015.

[39] S. Mun, S. Cho, M. Whang, B.-K. Ju, and M.-C. Park, "SSVEP-based BCI for manipulating three-dimensional contents and devices," *Proc. SPIE*, vol. 8384, pp. 189–196, May 2012.

[40] C. Han, G. Xu, Y. Jiang, H. Wang, X. Chen, K. Zhang, J. Xie, and F. Liu, "Stereoscopic motion perception research based on steady-state visual motion evoked potential," in *Proc. 41st Annu. Int. Conf. IEEE Eng. Med. Biol. Soc. (EMBC)*, Jul. 2019, pp. 3067–3070.

[41] J. Chen, M. Mcmanus, M. Valsecchi, L. R. Harris, and K. R. Gegenfurtner, "Steady-state visually evoked potentials reveal partial size constancy in early visual cortex," *J. Vis.*, vol. 19, no. 6, p. 8, Jun. 2019.

[42] A. Cotrina, A. B. Benevides, J. Castillo-Garcia, A. B. Benevides, D. Rojas-Vigo, A. Ferreira, and T. F. Bastos-Filho, "A SSVEP-BCI setup based on depth-of-field," *IEEE Trans. Neural Syst. Rehabil. Eng.*, vol. 25, no. 7, pp. 1047–1057, Jul. 2017.

[43] A. Floriano, D. Delisle-Rodriguez, P. F. Diez, and T. F. Bastos-Filho, "Assessment of high-frequency steady-state visual evoked potentials from below-the-hairline areas for a brain-computer interface based on depth-of-field," *Comput. Methods Programs Biomed.*, vol. 184, Feb. 2020, Art. no. 105271.

[44] B. Allison, T. Luth, D. Valbuena, A. Teymourian, I. Volosyak, and A. Graser, "BCI demographics: How many (and what kinds of) people can use an SSVEP BCI?" *IEEE Trans. Neural Syst. Rehabil. Eng.*, vol. 18, no. 2, pp. 107–116, Apr. 2010.

[45] Z. Lin, C. Zhang, W. Wu, and X. Gao, "Frequency recognition based on canonical correlation analysis for SSVEP-based BCIs," *IEEE Trans. Biomed. Eng.*, vol. 54, no. 6, pp. 1172–1176, Jun. 2007.

[46] D. J. McFarland and J. R. Wolpaw, "Brain-computer interfaces for communication and control," *Commun. ACM*, vol. 54, no. 5, pp. 60–66, 2011.

[47] X. Chen, B. Zhao, Y. Wang, S. Xu, and X. Gao, "Control of a 7-DOF robotic arm system with an SSVEP-based BCI," *Int. J. Neural Syst.*, vol. 28, no. 8, Oct. 2018, Art. no. 1850018.

[48] A. Floriano, P. F. Diez, and T. Freire Bastos-Filho, "Evaluating the influence of chromatic and luminance stimuli on SSVEPs from behind-the-ears and occipital areas," *Sensors*, vol. 18, no. 2, p. 615, Feb. 2018.

[49] X. Chen, Z. Chen, S. Gao, and X. Gao, "A high-ITR SSVEP-based BCI speller," *Brain-Comput. Interface*, vol. 1, nos. 3–4, pp. 181–191, Oct. 2014.

[50] B. Liu, X. Huang, Y. Wang, X. Chen, and X. Gao, "BETA: A large benchmark database toward SSVEP-BCI application," *Frontiers Neurosci.*, vol. 14, p. 627, Jun. 2020.

[51] F. Zhu, L. Jiang, G. Dong, X. Gao, and Y. Wang, "An open dataset for wearable SSVEP-based brain-computer interfaces," *Sensors*, vol. 21, no. 4, p. 1256, Feb. 2021.

[52] C. Farmaki, N. Zacharioudakis, M. Pediaditis, M. Krana, and V. Sakkalis, "Application of dry EEG electrodes on low-cost SSVEP-based BCI for robot navigation," in *Proc. IEEE Int. Conf. Imag. Syst. Techn. (IST)*, Jun. 2022, pp. 1–6.

[53] M. A. Pastor, J. Artieda, J. Arbizu, M. Valencia, and J. C. Masdeu, "Human cerebral activation during steady-state visual-evoked responses," *J. Neurosci.*, vol. 23, no. 37, pp. 11621–11627, Dec. 2003.

SYEDA R. ZEHRA (Graduate Student Member, IEEE) received the B.Eng. degree (Hons.) in biomedical engineering from the Swinburne University of Technology, Melbourne, VIC, Australia, in 2018. She is currently pursuing the Ph.D. degree in biomedical engineering with the ARC Training Centre in Cognitive Computing for Medical Technologies, The University of Melbourne, Melbourne. Her current research interests include brain–computer interfaces, assistive technologies, and advanced signal processing.

JING MU (Member, IEEE) received the B.Eng. degree in automotive engineering from the University of Shanghai for Science and Technology, Shanghai, China, in 2014, and the M.Eng. degree (Hons.) in mechatronics and the Ph.D. degree in brain–computer interface (BCI) from The University of Melbourne, Melbourne, VIC, Australia, in 2017 and 2023, respectively.

She is currently a Research Fellow with the Department of Biomedical Engineering, The University of Melbourne, and part of the ARC Training Centre in Cognitive Computing for Medical Technologies. Her current research interests include non-invasive BCIs, assistive technologies, and robotics.

BRANDON V. SYIEM received the B.Tech. degree from North-Eastern Hill University, India, in 2014, and the M.Sc. and Ph.D. degrees in computer science from The University of Melbourne, Australia, in 2017 and 2023, respectively. He is currently a Postdoctoral Research Fellow with the Queensland University of Technology. His research interests include the intersection of extended reality (XR), artificial intelligence (AI), and cognitive psychology.

ANTHONY N. BURKITT (Senior Member, IEEE) received the B.Sc. degree in theoretical physics from The Australian National University, Canberra, Australia, in 1980, and the Ph.D. degree in theoretical physics from The University of Edinburgh, Edinburgh, U.K., in 1983.

He held a postdoctoral research positions with the University of Liverpool, U.K., the University of Wuppertal, Germany, The Australian National University, and the Bionics Institute, Melbourne, VIC, Australia. Since 2007, he has been holding the Chair of Bio-Signals and Bio-Systems with the Department of Biomedical Engineering, The University of Melbourne, Melbourne, where he is currently a Full Professor. He was the Director of Bionic Vision Australia (2010–2016), a Special Research Initiative in Bionic Vision Science and Technology of the Australian Research Council (ARC). He has authored more than 130 articles in peer-reviewed international journals. His research interests include computational neuroscience, neuroengineering, retinal implants, brain–computer interfaces (BCIs), cochlear implant speech processing, and bio-signal processing for epilepsy. He received the 2019 Victoria Prize for Science & Innovation in the Physical Sciences, the 2019 Eureka Prize for Excellence in Interdisciplinary Scientific Research, and the 2018 Royal Society of Victoria Medal for Excellence in Scientific Research.

DAVID B. GRAYDEN (Senior Member, IEEE) received the B.E. degree (Hons.) in electrical and electronic engineering, the B.Sc. degree in computer science, and the Ph.D. degree in electrical and electronic engineering from The University of Melbourne, Melbourne, VIC, Australia, in 1990, 1991, and 1999, respectively. From 1997 to 2006, he held a postdoctoral research position with the Bionics Institute, East Melbourne, VIC, Australia. Since 2006, he has been an Academician with The University of Melbourne, where he is currently a Full Professor and the Clifford Chair of Neural Engineering, Department of Biomedical Engineering. He was the inaugural Head of the Department of Biomedical Engineering, from 2017 to 2019. He has authored more than 150 articles in peer-reviewed international journals and book chapters. His research interests include brain–computer interfaces, computational neuroscience, and medical bionics, including cochlear, retinal, brain, and peripheral neural stimulation. He was the 2020–2021 IEEE EMBS Distinguished Lecturer and the 2021 Norman Curry Award for Innovation and Excellence in Educations Programs, the 2019 Eureka Prize for Excellence in Interdisciplinary Scientific Research, and the 2019 Melbourne School of Engineering Award for Outstanding Graduate Researcher Supervision.

● ● ●